Quaternary Science Reviews 225 (2019) 106004

Contents lists available at ScienceDirect

Quaternary Science Reviews

journal homepage: www.elsevier.com/locate/quascirev

Atmospheric response to mid-Holocene warming in the northeastern Atlantic: Implications for future storminess in the Ireland/UK region

Michelle J. Curran [a, *], Yair Rosenthal [b], James D. Wright [c], Audrey Morley [a, d]

[a] School of Geography and Archaeology and The Ryan Institute at the National University of Ireland Galway, Ireland
[b] Department of Marine and Coastal Sciences and Department of Earth and Planetary Sciences, Rutgers, The State University of New Jersey, 71 Dudley Road, New Brunswick, NJ 08901, USA
[c] Department of Earth and Planetary Sciences, Rutgers, The State University of New Jersey, 71 Dudley Road, New Brunswick, NJ 08901, USA
[d] iCRAG – Irish Centre for Research in Applied Geosciences, Ireland

ARTICLE INFO

Article history:
Received 1 July 2019
Received in revised form
15 October 2019
Accepted 15 October 2019
Available online xxx

Keywords:
Holocene
Paleoceanography
North Atlantic
Organic geochemistry
Foraminifers

ABSTRACT

There is increasing evidence that accelerated warming at high-latitudes is associated with increased climate variability at mid-latitudes, including the frequency and intensity of storms. However, due to short instrumental records our understanding of how ocean-atmosphere dynamics operate during warmer than present climates remains limited. Here we present a palaeoceanographic investigation of the transition between the middle Holocene intervals of the Northgrippian (8.2–4.2 ka) and the late Holocene interval of the Meghalayan (4.2–0 ka) to test the hypothesis of an eastward shift of the Icelandic Low under warmer than present climate scenarios. Reconstructions of bottom water temperatures (BWT) and stable oxygen isotopes (Mg/Ca, $\delta^{18}O$) using the benthic foraminifera *Hyalinea balthica* reveal warmer than present BWT of up to 2.6 ± 0.7 °C on the Irish Continental Shelf until circa 4.2 ka. The results suggest that Atlantic waters of subtropical origins were more prevalent in the eastern subpolar gyre (SPG) and on the Irish Continental Shelf. We link this oceanographic signature to an eastward shift of the Icelandic Low. We then place our local temperature record into an extra-regional context, using a combination of modern observations and existing palaeo datasets, which enables us to assess the impact of changing atmospheric modes on ocean-atmosphere climate linkages within the North Atlantic Region. The enhanced influence of warm subtropical Atlantic waters recirculating along the boundaries of the SPG under this scenario, would potentially have enhanced melt rates of marine-terminating glaciers on the east Greenland Shelf during the Northgrippian.

1. Introduction

The Icelandic Low is a large-scale persistent atmospheric centre of low-pressure and its strength and position within the subpolar North Atlantic determine storm trajectories and intensities during winter months (Feser et al., 2014). In response to future warming and a reduced latitudinal temperature gradient, multiple climate models are predicting an eastward shift of the Icelandic Low from its predominant position over the Irminger Sea Basin to the Southern Nordic Seas (Pinto et al., 2009; Ulbrich and Christoph, 1999). Moreover, a climate model by Zappa et al. (2013) predict an increase in storm track density and amplification of strong cyclones close to the British Isles, further indication of an eastward positioning of the Icelandic Low. Thus, an increase in storm intensities and frequencies is expected for the Ireland/UK region due to the closer proximity of the centre of low-pressure systems (Pinto et al., 2009). Moreover, the frequency of extreme precipitation events are also projected to increase for Ireland (Steele-Dunne et al., 2008). However, it remains unknown whether this atmospheric signature outlined for the future is recorded by long-term climate observations of warmer than present environments, for example during the Northgrippian stage (8.2–4.2 ka) of the Holocene Epoch (Walker et al., 2018). If so, a comprehensive understanding of ocean-atmosphere climate linkages during the Northgrippian at regional scales could provide a powerful tool to estimate and prepare for future climate change in north-western (NW) Europe and beyond. This is important, as a shift of the Icelandic Low is most likely to affect surface ocean properties and

* Corresponding author.
E-mail address: m.curran18@nuigalway.ie (M.J. Curran).

https://doi.org/10.1016/j.quascirev.2019.106004
0277-3791/

frontal systems that control coastal climates and ecosystems (Le Mezo et al., 2016; Reverdin et al., 2018).

At subpolar latitudes of the North Atlantic Region, the Northgrippian is generally the warmest of the three stages that define the Holocene epoch: the Greenlandian (11.7–8.2 ka), the Northgrippian (8.2–4.2 ka) and the Meghalayan (4.2–0 ka) (Walker et al., 2018). The late regional onset of peak warming during the Northgrippian was due to the strong ice-albedo effect and the slow demise of Northern Hemisphere ice-sheets at the end of the Greenlandian (Kutzbach and Webb, 1993). As a result, the timing, duration and magnitude of peak warming is regionally specific (Came et al., 2007; Charpentier Ljungqvist, 2011). At subpolar latitudes in the North Atlantic Basin, peak warming of the Northgrippian (Wanner et al., 2015) occurred between ~7 and 4 ka and resulted in sea surface temperatures (SST) ~2 °C warmer than present (Came et al., 2007; Marcott et al., 2013; Morley et al., 2014). High Arctic warming, reduced sea-ice extent (especially in the Barents Sea), and overall weaker latitudinal temperature gradient (Davis and Brewer, 2009; Stranne et al., 2014; Zhang et al., 2010) thus make the Northgrippian an interesting case study to evaluate the impact of future warming on ocean-atmosphere climate dynamics over the North Atlantic Basin.

Our current understanding of the mechanisms that control the interactions between the atmosphere and the North Atlantic Ocean on interannual to multidecadal timescales relies on early work by Bjerknes (1964), who suggested that while atmospheric processes force interannual variability in SST, oceanic processes drive multidecadal SST and likely atmospheric variability on multidecadal timescales. This hypothesis is supported by observational evidence (Gulev et al., 2013) and combined observational/reanalysis data and modelling (Knight et al., 2006; Peings and Magnusdottir, 2014; Zhang et al., 2007), suggesting that multidecadal (50–70 year) patterns of atmospheric circulation (e.g. the North Atlantic Oscillation - NAO) are forced by the ocean (Peings and Magnusdottir, 2014).

Spatial observations of SST in the North Atlantic Basin (1870s–2000s) demonstrate that on multidecadal timescales a tripole pattern, referred to as the Atlantic Multidecadal Oscillation (AMO), dominates SST variability on ~50–70 year timescales (Cunningham et al., 2013; Hall et al., 2015; Knight et al., 2005; Pinto and Raible, 2012). During positive phases (AMO +) anomalously warm SST dominate, while during negative phases (AMO -) anomalously cool SST occupy the subpolar North Atlantic Basin (Knight et al., 2005). Typically, AMO + (AMO -) phases coincide with a weakened (strengthened) subpolar gyre (SPG) circulation (Holliday, 2003), and reduced (enhanced) heat exchange with the atmosphere, which results in cooler (warmer) climates in NW Europe.

The atmospheric counterpart to the AMO is often simplified into a multidecadal expression of the NAO (Peings and Magnusdottir, 2014; Pinto and Raible, 2012). The NAO is a station-based index that records sea-level pressure differences between Reykjavik (Iceland) and Lisbon (Portugal) (Hurrell, 1995; Osborn, 2006). However, the traditional two-point NAO index does not fully capture the basin-scale variability (Curry and McCartney, 2001) as it assumes that the centres of action, the Icelandic Low and the Azores High, are spatially fixed (Curry and McCartney, 2001; Hall et al., 2015; Moore et al., 2013). More accurately, it is the combined interaction of the NAO (accounting for ~40% of winter variance) (Hurrell et al., 2003), the East Atlantic pattern (EA) and the Scandinavian pattern (SCA) that describes climate variability within the North Atlantic Region (Moore et al., 2013). The EA, first proposed by Wallace and Gutzler (1981) is best described by a monopole low-pressure system located approximately 52°N – 55°N, west of Ireland (Barnston and Livezey, 1987; Hall et al., 2015; Moore and Renfrew, 2012; Moore et al., 2013). To date relatively little research focuses on the forcing and climatic impacts of the EA (Moore et al., 2011). Due to this scarcity, the mechanism of how the EA operates remains ambiguous. For example, a series of publications by Moore et al. propose that the combination of positive (opposite) EA and the NAO phases, result in a southward (northward) shift and intensification (decrease) of the Icelandic Low (Moore and Renfrew, 2012; Moore et al., 2011, 2013). Alternatively, Comas-Bru and McDermott (2014) link the southward migration of the NAO dipole to an opposite phase relationship between the NAO and EA. While the phase relationship between the NAO and EA remains debated, there is some consensus that the EA manifests in combination with the NAO and results in a southward migration of the Icelandic Low to the west of Ireland (Comas-Bru and McDermott, 2014; Moore and Renfrew, 2012; Moore et al., 2011, 2013; Ruprich-Robert and Cassou, 2015; Woollings et al., 2010). Moore et al. (2011) provide evidence from 2007 that during positive phases of both the NAO (NAO +) and EA (EA +) the Icelandic Low was moved southward and increased in intensity, resulting in increased storminess for the British Isles. This situation (NAO + and EA +) occurs ~27% of the time (Moore et al., 2011). Here we infer that the closer proximity of the centre of low pressure to the Irish coast during the EA + pattern would likely result in intense local westerly winds (Table 1).

The SCA is characterised by a primary low-pressure system located to the west of Bergen, Norway (Barnston and Livezey, 1987; Hall et al., 2015; Moore et al., 2013) in combination with the Siberian High located over eastern Europe/western Russia (Bueh and Nakamura, 2007; Rodriguez-Puebla et al., 1998). A positive phase of the SCA (SCA +) result in above average precipitation conditions across southern Europe and the UK region and anomalously low precipitation over the Scandinavian Peninsula (Bueh and Nakamura, 2007) and are likely to result in predominant westerlies off the west coast of Ireland (Table 1) due to the position of the high and low pressure systems. During negative phases of the SCA (SCA -) the storm track is extended north-eastward towards Scandinavia resulting in warmer conditions over the area (Bueh and Nakamura, 2007). The interaction of these three modes highlights the mobility of the primary centres of action within the North Atlantic Region (Hall et al., 2015; Moore et al., 2013) and underlines that a station-based index such as the NAO may be too simplistic when assessing ocean-atmosphere climate linkages. For example, the distribution and strength of the East Greenland (EGC) and Irminger Currents (IC) fluctuate in response to the location and intensity of the Icelandic Low (Blindheim and Malmberg, 2005; Dickson et al., 2002).

Often, interpretations of past climate records tend to focus on the multidecadal expression of the NAO to explain the proxy data (Pinto and Raible, 2012; Vinther et al., 2010). Given the actual variability of atmospheric modes it is not surprising that this approach has led to significant uncertainties in palaeo-NAO reconstructions and to contradictory interpretations of past atmospheric variability over the North Atlantic Basin (Giraudeau et al., 2010; Müller et al., 2012; Trouet et al., 2012), especially during the Northgrippian when the typical NAO dipole cannot reconcile all observations made in the North Atlantic Region (Morley et al., 2014).

Here we present a palaeoceanographic investigation of the transition between the Northgrippian (8.2–4.2 ka) and the Meghalayan (4.2–0 ka) to test the hypothesis that variations in atmospheric modes affect regional oceanographic conditions on the Irish Continental Shelf. To evaluate this hypothesis we present a combination of modern observations alongside a 7.5 ka long palaeoceanographic record collected from the Irish Continental Shelf. We then place this local record into an extra-regional context,

Table 1
Approximate location of the Icelandic Low and strength during modes of the North Atlantic Oscillation (NAO), Scandinavian pattern (SCA) and East Atlantic pattern (EA) (Hurrell, 1995; Moore et al., 2013). Also stated are prevailing wind directions for Ireland associated with each atmospheric configuration, the likelihood of storm intensity/frequency for Ireland and the British Isles and the relative strength of the EGC (East Greenland Current) and the IC (Irminger Current) (Blindheim and Malmberg, 2005; Dickson et al., 2002).

Atmospheric mode	Icelandic Low location	Icelandic Low strength	Prevailing wind direction	Storm intensity/ frequency	Strength of EGC/IC
SCA	West of Bergen, (Norway)	Strong	Predominant westerlies	Increased	EGC (−)/IC (+)
EA	West of Ireland	Strong	Predominant westerlies	Increased	EGC (−)/IC (+)
NAO +	Irminger Sea Basin	Strong	Strong south-westerlies	Increased	EGC (+)/IC (−)
NAO -	Irminger Sea Basin	Weak	Weak south-westerlies	Decreased	EGC (−)/IC (+)

which enables us to assess the impact of a warmer climate on ocean-atmosphere climate linkages in the North Atlantic Region.

2. Material and methods

2.1. Oceanographic setting

Core CV15025_GC_07_01 (hereinafter GC07) was retrieved from the Dingle-Shannon Basin site at 52°58.46 N, 9°57.56 W, 110 m below sea-level (m) during *R/V Celtic Voyager* cruise CV15025 in October 2015 (Fig. 1). The bathymetry of the Irish Continental Shelf typically plateaus rapidly to 80–100 m within 20 km from the coast (Fernand et al., 2006). Thereafter it extends to the shelf edge as a relatively level plane. GC07 is situated within the Irish Coastal Current (ICC) system that transports relatively fresh and cool coastal waters northwards from the Bay of Biscay (Aquitaine/Armorican Shelf), hugging the coastlines of France, southern UK and Ireland (Pingree and Lecann, 1989; Raine, 2014; Raine et al., 2002). The main freshwater sources reaching the site via the ICC are the river outflows of the Loire in France, Severn in the UK, and more locally the Shannon in Ireland (Nolan and Lyons, 2006). Generally, tidal amplitudes on the western Irish Continental Shelf are weak, as such wind-mixing dominates over tidal-mixing (Fernand et al., 2006). There is evidence to support the development of a summer thermocline at ~35–40 m water depth (Raine et al., 1993). However, at 110 m, the core site is below the seasonal mixed layer depth where inter-seasonal temperature variability does not alter bottom water temperature (BWT). Instead BWT are determined by surface heat exchange during the winter (Hill et al., 2008; Scott et al., 2003; Scourse and Austin, 2002) and thus reflect winter conditions. Modern BWT and salinity at the core site during October are 11.5 °C and 35.5, respectively. The reader is referred to the supplementary section for supporting CTD data.

Atlantic waters in the eastern North Atlantic are of two main origins: The North Atlantic Current (NAC) originating in the Gulf of Mexico (Sutton and Allen, 1997) and subtropical gyre (STG) sourced waters (Hátún et al., 2005). The relative contribution of each water mass is governed by dynamic changes in the SPG and the STG (Hátún et al., 2005). Thus the site of GC07 is influenced by the varying modes of the SPG and STG and ICC waters, which depend of the background atmospheric modes in the North Atlantic. During AMO + (AMO -) like conditions, a weakened (strengthened) SPG (STG) results in the prevalence of relatively warmer (cooler) STG sourced (NAC) waters in the eastern Subpolar North Atlantic (Hátún et al., 2005).

A perennial salinity front, the Irish Shelf Front, exists to the west

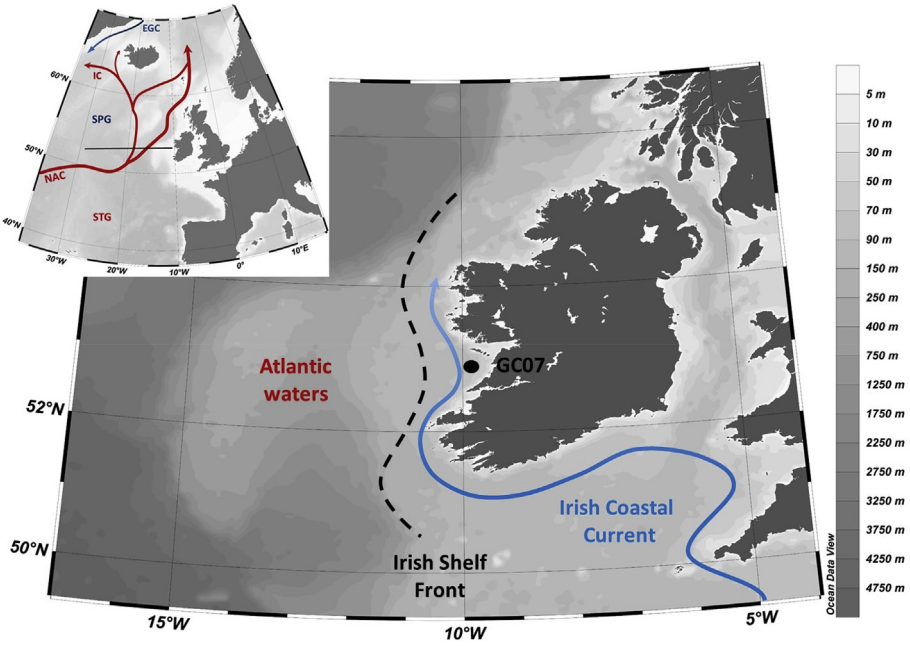

Fig. 1. Map of core location (GC07 52°58.46 N, 9°57.56 W, 110 m depth) marked by a black circle. The grey scale signifies bathymetry. Also shown is a schematic representation of the Irish Coastal Current (ICC) and the Irish Shelf Front (dashed black line). The inset shows a schematic representation of the North Atlantic Current (NAC), the Irminger Current (IC) and the East Greenland Current (EGC). Also shown are relative locations of the Subpolar Gyre (SPG) and the Subtropical Gyre (STG). The black line marks the cross section for temperature and salinity plots in Fig. 2.

of the core site (Huang et al., 1991). The front is characterised as a 'Type I' front that extends from the sea-surface to the sea-floor (McMahon et al., 1995; Raine and McMahon, 1998). It separates the relatively cool and fresh (<35.0) waters of the ICC from more saline Atlantic waters (>35.3) (Fig. 2) (McMahon et al., 1995; Raine, 2014; Raine and McMahon, 1998; Raine et al., 2002). From observational evidence, Raine and McMahon (1998) show mobility of the Irish Shelf Front as a result of prevailing wind direction, with a more westerly wind driving the Irish Shelf Front closer to the coast.

2.2. Paired Mg/Ca–$\delta^{18}O$ measurements

We reconstructed BWT and salinities over the past 7.5 ka by measuring Mg/Ca and stable oxygen isotopic values ($\delta^{18}O_c$) on the benthic foraminifera *Hyalinea balthica*. *Hyalinea balthica* is a shallow infaunal benthic foraminifera favouring fine-grained sediments (Rosenthal et al., 2011; Villanueva Guimerans and Cervera Currado, 1999). *Hyalinea balthica* can be found worldwide in shallow to intermediate waters (primarily <600 m depth) and are most abundant in cool North Atlantic waters ranging between ~4 °C–12 °C (Rosenthal et al., 2011). The high temperature sensitivity and low uncertainties for reconstructed temperatures (±0.7 °C) make it ideal for high-resolution reconstruction of past BWT (Rosenthal et al., 2011).

Up to 40 tests from the 250–355 μm size fraction were prepared for trace element analysis, following a modified reductive, oxidative cleaning protocol (Rosenthal et al., 1997). This includes the removal of clays, metal oxides, and organic matter from crushed shells. The prepared samples were then analysed at Rutgers Inorganic Analytical Laboratory using a Finnegan MAT Element XR Sector Field Inductively Coupled Plasma Mass Spectrometer (ICP-MS) following the methods outlined in Rosenthal et al. (1999). The long-term analytical precision of Mg/Ca ratios is based on three consistency standards of Mg/Ca concentrations of 1.44, 3.49, and 8.70 mmol mol^{-1}. Over the course of this study, the precision for the consistency standards was 0.35, 0.43, and 0.21% RSD (relative standard deviation) respectively. To convert molar mass ratios into palaeotemperatures we followed Rosenthal et al. (2011).

$$Mg/Ca = 0.49\,T\,(^{\circ}C) \quad (1)$$

For $\delta^{18}O_c$ analysis eight foraminiferal shells were crushed between two glass plates to aid the removal of clays prior to analysis at the Department of Earth and Planetary Sciences at Rutgers University, using Micromass Optima mass spectrometer fitted with a Multiprep device and reported against Vienna Pee Dee Belemnite (VPDB).

In order to determine the most suitable equation for the reconstruction of oxygen isotopes of seawater ($\delta^{18}O_{sw}$) at our core site we tested five independent palaeotemperature equations (Bemis et al., 1998; Lynch-Stieglitz et al., 1999; Marchitto et al., 2014; Shackleton, 1974) on *Hyalinea balthica* specimen collected from the 0–0.5 cm interval of a box core taken at the same time as the gravity core at site GC07. To correctly assess $\delta^{18}O_{sw}$ we calculated the $\delta^{18}O_c$ offset from equilibrium for each equation following Rosenthal et al. (2011). The reader is referred to the supplementary section for full details. The core top Mg/Ca value is 5.79 μmol.mol-1 and corresponds to a bottom water temperature of 11.59 °C using equation (1) and the paired $\delta^{18}O_c$ value is 1.09‰. Equations developed for deep-water benthic foraminifera (Shackleton, 1974) yield $\delta^{18}O_{sw}$ values that are too high when compared to modern conditions (see Table A2 in supplementary section). Applying the equation developed by Bemis et al. (1998) for low light planktonic foraminifera and including a vital effect of 0.22‰ calculated following Rosenthal et al. (2011) affords more realistic values (i.e. $\delta^{18}O_{sw} = 0.49‰$) given modern observations Austin et al. (2006).

$$\delta^{18}O_{sw} = 0.27 + \left(\left(\left(\delta^{18}O_c + 0.22\right)*4.8\right) + T - 16.5\right)/4.8$$
$$\delta^{18}O_{sw}\left(VPDB\right) = \delta^{18}O_{sw}\left(VSMOW\right) - 0.27 \quad (2)$$

where T represents temperature (in °C) derived from Mg/Ca measurements, $\delta^{18}O_{sw}(VSMOW) = m*S - c$ (where m is the salinity:$\delta^{18}O$ mixing line gradient, S is the salinity and c is the intercept) and $\delta^{18}O_c$ and $\delta^{18}O_{sw}$, the isotopic composition in δ -units (i.e., % deviation of $^{18}O/^{16}O$ ratio vs. standard value) of, respectively, calcite (measured against VPDB), and ambient water (measured against VSMOW). Calculations were completed by subtracting 0.27‰ in order to compare measured $\delta^{18}O$ values of CO_2 produced by the reaction of calcite with H_3PO_4 and CO_2 equilibrated with water (Friedman and O'Neil, 1977).

For the conversion of $\delta^{18}O_{sw}$ into salinity we selected equation two developed by Austin et al. (2006) for the west of Scotland and Ireland and the South West Approaches, where bottom water salinities are ≥35.

$$\delta^{18}O_{sw} = \left(S*0.597\right) - 20.685 \quad (3)$$

Where S = salinity and $\delta^{18}O_{sw}(VPDB) = \delta^{18}O_{sw}(VSMOW) - 0.27$. Application of Eq. (3) to downcore $\delta^{18}O_{sw}$ values provides average reconstructed salinity value of 35.6 (±0.69). Comparison to modern distribution of salinity values at 110 m water depth reveal these fall within existing values for water originating from subpolar and subtropical origins. Standard-error estimates for palaeotemperature, $\delta^{18}O_c$, $\delta^{18}O_{sw}$ and are ±0.7 °C, ± 0.07‰, ±0.3‰ and ±0.69 respectively (Bamberg et al., 2010; Rosenthal et al., 2011).

3. Chronology

The age model for GC07 (Fig. 3) is constrained by eight

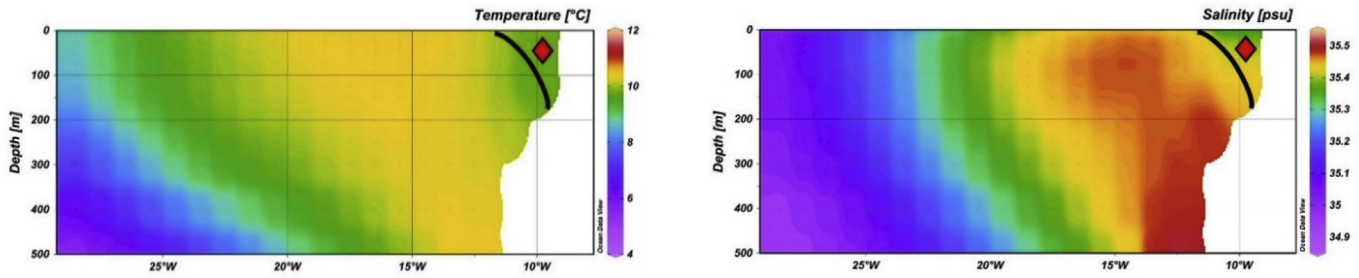

Fig. 2. Modern temperature and salinity plots taken from Ocean Data View World Ocean Database (Available at: https://odv.awi.de/data/ocean/world-ocean-atlas-2009). Also shown is a schematic representation of the Irish Shelf Front in black and the location of GC07 marked by a diamond.

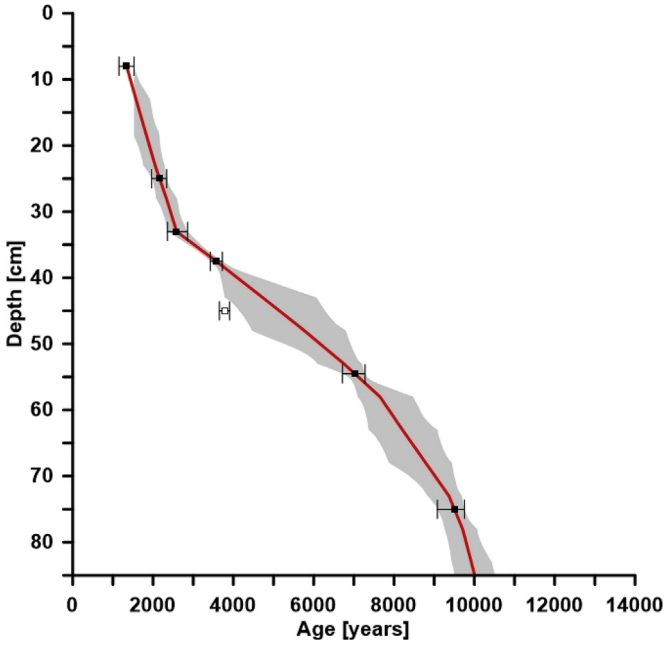

Fig. 3. Age model GC07 we show the age-depth relationship between calibrated AMS ^{14}C radiocarbon dates (±2σ) (black) and depth for the top 80 cm of the core, with errors shown in grey shading. Also shown is the excluded GC45 (white). Six of the eight AMS ^{14}C dates (Table 2) included in the age model fall within the past 7.5 ka.

Accelerator Mass Spectrometry (AMS) radiocarbon measurements (^{14}C) measured at the Keck Carbon Cycle AMS facility at UC Irvine, USA (a) and the Radiocarbon Dating Facility Queens University, Belfast, UK (b). The samples consist of a minimum of 3 mg undamaged, benthic foraminiferal shells including *Hyalinea balthica (H. balthica), Quinqueloculina semulina (Q. semulina)* and *Ammonia beccarii (A. beccarii)*. Individuals were picked at 8, 25, 33, 37.5, 45, 65.4, 75 and 156 cm respectively (Table 2). All radiocarbon dates were converted to calendar years with the MARINE 13 calibration dataset (Stuiver and Reimer, 1993). We applied a regional Marine Reservoir Effect (MRE) developed for Ireland and the British Isles by Ascough et al. (2009) to estimate ΔR values for each date in our chronology. ΔR values were compiled from several papers using the multiple paired sample approach to extend ΔR values for the Holocene period (Ascough et al., 2009). We then proceeded to include these ΔR values in our Bayesian age model using the Bacon software package (Blaauw and Christen, 2013). Error estimates for each sample at 95% confidence intervals were calculated using Bacon 2.2, Bayesian age-depth modelling software. The following prior values (accumulation shape = 1.5, accumulation mean = 100 years/cm, memory strength = 4, memory mean = 0.7) were used to begin the Markov Chain Monte Carlo iterations. At 0 cm the model estimates an age of 941 ka BP indicating that modern sediments are missing, which is not unusual as these softer sediments are frequently lost during core recovery. Table 2 reports the weighted mean averages (WMA) of the calibrated probability distribution for each age with their respective 2σ confidence range. Over the course of the Holocene, we note three changes in the local sedimentation regimes. Between 13 ka and 9.5 ka sedimentation rates were high at ca. 42 years per cm. From 9.5 ka to 2.5 ka, sedimentation rates decreased to 168 years per cm and increased again to 75 years per cm after 2.5 ka. Modern sedimentation rates as determined from a box core by Martin et al. (2017) are similar to the past 2.5 years and on the order of 80 yr per cm. Today the core site GC07 is situated below the seasonal mixed layer depth, however we cannot dismiss the possibility of a change in sedimentation rate due to increased storminess and a deepening of the mixed layer depth which may have resulted in winnowing. Sampling resolution for GC07 was at 0.5 cm. We acknowledge that at this high-resolution it is inevitable that bioturbation results in a smoothing of the climate signature, particularly during periods of low sediment accumulation (Anderson, 2001). Therefore, interpretation of the final dataset focuses on centennial to millennial-scale changes, with the exception of a short interval during the Meghalayan, the Roman Warm Period (RWP) centred ~2.4 ± 0.2 ka, when sedimentation rates allow for an assessment of the multidecadal variability in the dataset. We generated a 200-year low-pass filter to all time series and provide the filters' error envelopes. These were determined by calculating the standard error of the mean (e.g. 200-year low pass filter) (Fig. 4), which takes into account changes in sedimentation rate.

4. Results

4.1. Geochemical analysis on GC07

Unless stated otherwise, all results and uncertainties reported here refer to the 200-year low pass filter. Mg/Ca measurements from gravity core GC07 indicate a gradual warming from 11.5 °C at 7.5 ± 0.2 ka to reach a maximum of 13.1 °C at 4.2 ± 0.2 ka (Fig. 4a). This warm phase is followed by a distinct cooling trend into the Meghalayan. This trend is gradual between 4.2 and 2.4 ka and thereafter more abrupt, culminating in minimum temperatures of 10.4 °C at 1.0 ± 0.051 ka. The record reveals marked centennial to

Table 2
AMS ^{14}C radiocarbon dates for GC07. ^{14}C measurements run at a) the Keck Carbon Cycle AMS facility at UC Irvine, USA and b) the Radiocarbon Dating Facility Queens University, Belfast, UK. *WMA = Weighted Mean Average. GC45 was excluded from the age model as the inclusion of this date in the age model would have resulted in unrealistic sedimentation rates which suggests that the age is slightly too young (Fig. 3). The strong agreement of two dates measured at 37.5 validates the omission of GC45. It is likely the offset in the date at 45 cm is an artefact of bioturbation, which may occur, particularly in low sedimentation environments (Anderson, 2001). **UCIAMS-169782 is from a previous study by Martin et al. (2017). The box core was taken at the same time and location as GC07 and had an intact water-sediment interface. We consider the top 0–0.5 cm as modern.

Lab ID	Core depth (cm)	Benthic foraminifer	Radiocarbon age ±1σ error (yr BP)	Calibrated age WMA* (cal. ka BP)	ΔR values following Ascough et at. (2009)	Δ SD	2σ range (cal. ka BP)
UCIAMS-169786[a]	8	*H. balthica*	1710 ± 15	1342	−94.90	0	1153–1525
UCIAMS-179346[a]	25	*H. balthica*	2380 ± 20	2163	−111.45	60	1965–2339
UBA-36160[b]	33	*Q. semulina, H. balthica*	2734 ± 29	2586	−107.34	60	2361–2858
UCIAMS-193990[a]	37.5	*H. balthica, A. beccarii, Q. seminulum*	3670 ± 20	3571	−77.67	60	3727–3569
GC37.5b	37.5	*Q. seminulum*	3600 ± 20	3571	−77.67	60	3727–3569
UBA-36161[b]	45	*H. balthica, A. beccarii, Q. seminulum*	3790 ± 41	N/A	N/A	N/A	N/A
UCIAMS-179347[a]	54.5	*Q. semulina, H. balthica*	6655 ± 25	7022	88.64	60	6717–7278
UCIAMS-169788[a]	75	*Q. semulina, A. beccarii*	8735 ± 20	9504	−127.10	60	9081–9756
UCIAMS-169788[a]	156	*Q. semulina*	11295 ± 35	12932	0	60	12654-13337
*UCIAMS-169782***	*14*	*H. balthica*	*1565 ± 15*	*1125*	-	-	*1051–1187*

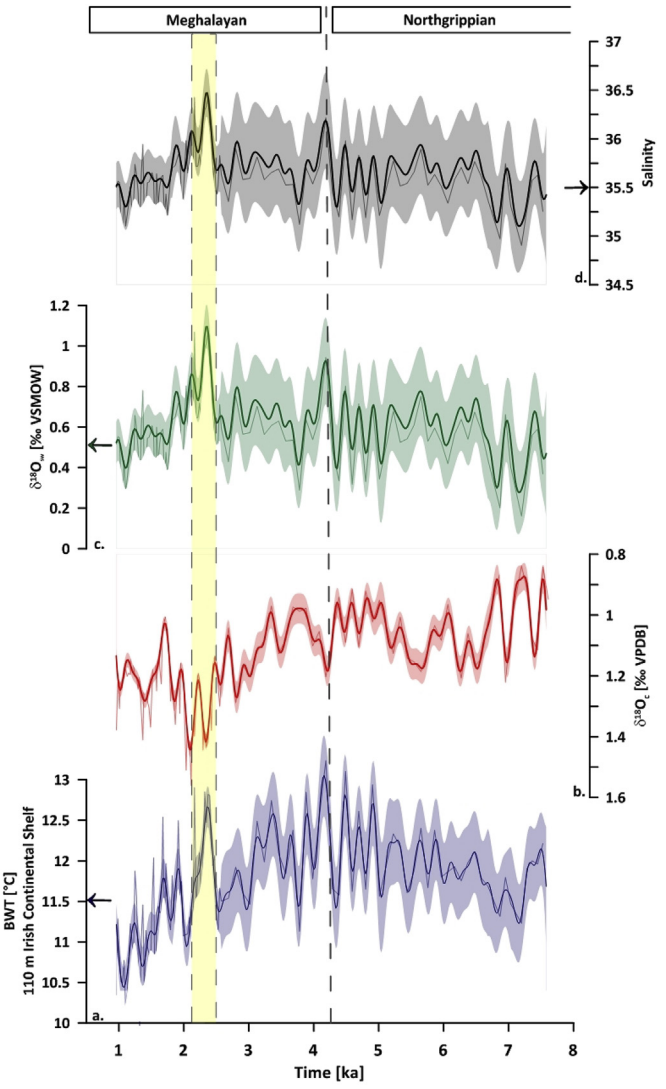

Fig. 4. Results. All graphs are plotted versus age and 200-year low-pass filter shown in bold. Also shown are the error envelopes for all 200-year low-pass filtered time series. a: Mg/Ca based BWT. b: measured $\delta^{18}O_c$ values ($\delta^{18}O_C$ ‰ relative to VPDB). c: calculated $\delta\ ^{18}O_{sw}$ derived from paired Mg/Ca - $\delta^{18}O$ measurements ($\delta^{18}O_{sw}$ ‰ relative to VSMOW). d: salinity derived from calculated $\delta\ ^{18}O_{sw}$ values. Also shown are the error envelopes for all 200-year low-pass filtered time series. The grey dashed line delineates the Northgrippian – Meghalayan transition. The highlighted area represents the Roman Warm Period (RWP) discussed in the text below. Arrows on y-axis indicate modern values for BWT, $\delta^{18}O_{sw}$ and salinity at the core site.

millennial scale BWT variability of roughly ±2.6 °C, which exceed the uncertainty of ±0.7 °C associated with palaeotemperature reconstructions. The intervals of warmest BWT occurred between ca. 4–5 ka and between 2.2 ± 0.1 ka – 2.4 ± 0.2 ka. Thereafter multidecadal cold events are centred at 1.4 ± 0.1 ka (10.7 °C) and 1 ± 0.05 ka (Fig. 4a).

The $\delta^{18}O_c$ values range between 0.87‰–1.44‰ (Fig. 4b), after correction for minor changes in ice volume following Fairbanks (1989) during the past 7.5 ka. When combined with palaeotemperatures, $\delta^{18}O_{sw}$ values reported in Vienna Standard Mean Ocean Water (VSMOW), reveal centennial scale variability over the duration of the record. $\delta^{18}O_{sw}$ values range between 0.28‰ at 7.2 ± 0.2 ka and 1.10‰ at 2.4 ± 0.2 ka, which correspond to 35.1 and 36.5, respectively.

5. Discussion

In the following discussion we evaluate our results to assess the oceanographic response at the eastern margin of the SPG to the Northgrippian – Meghalayan transition and then link these changes to past and possibly future large-scale ocean-atmospheric variability in the North Atlantic Region. In the first instance, we discuss our results for the Northgrippian in the context of modern observations and existing palaeoceanographic records in the subpolar North Atlantic and then proceed to offer a unifying interpretation for observations made within the region.

Based on our record the regional climate optimum in the eastern SPG occurred between ~5 and 4 ka. Prior to this BWT on the Irish Continental Shelf gradually increased from 7.5 ka onwards to reach maximum temperatures at 4.2 ka. There are three possible origins for the observed increase in BWT during this period. First, coastal waters transported northwards by the ICC may have been warmer during the Northgrippian. Alternatively, Atlantic waters transported via the NAC may have been warmer, or the contribution of Atlantic waters at the core site may have been greater. There has been much discussion on the contradictory temperature signals recorded by alkenone and foraminiferal based reconstructions during the Holocene (Came et al., 2007; Farmer et al., 2008; Laepple and Lohmann, 2009; Leduc et al., 2010; Liu et al., 2014; Risebrobakken et al., 2003). Alkenone-based records suggest a long-term cooling throughout the Holocene, while some foraminiferal-based records indicate a general long-term warming. Liu et al. (2014) and Farmer et al. (2008) suggest this difference in signal is the result of different habitat depth, which capture contrasting seasonal signals. SSTs are captured by phytoplankton-based alkenone records, which are dominated by summer insolation that decreased over the Holocene in the Northern Hemisphere. Conversely, winter insolation increased over the same period. Foraminifera that live in the subsurface and are therefore more likely to record changes in winter or annual temperature. As a result of this seasonal influence on the palaeotemperature signal and given that core site GC07 also records a winter signal only foraminifera-based records are considered in this study, unless otherwise stated.

5.1. Warmer ICC waters during the Northgrippian (8.2–4.2 ka)

Modern ICC waters are cooler and less saline than open Atlantic waters (McMahon et al., 1995; Raine, 2014; Raine and McMahon, 1998; Raine et al., 2002) as they are influenced by inflow from the Rivers Shannon, Severn and Loire (Nolan and Lyons, 2006). It is plausible that increased Surface Air Temperatures (SAT) during the Northgrippian could have increased river temperatures (Van Vliet et al., 2011) and resulted in warmer discharges to the ICC. However, many factors may influence stream temperature, including distance from the source of the stream, temperature of incoming water (precipitation, surface runoff, groundwater), and heating and cooling by heat exchange at the water/air interface (Morrill et al., 2005). Here we are evaluating the latter as a potential source for the warmer temperatures recorded on the Irish Continental Shelf.

Based on modern observations (1980s onwards) warmer winter (DJF) SST on the Irish Continental Shelf (Kaplan et al., 1998) coincide with increased SAT and enhanced precipitation (MET Éireann, 2018) in Ireland (Fig. 5). This is because warmer SAT are directly linked to the passage of mid-latitude cyclones over Ireland (Sweeney, 2014). A recent example of this occurred during the winter of 2013/14, one of the stormiest on record for the British-Irish Isles (Huntingford et al., 2014), when Ireland also experienced above average SAT (Matthews et al., 2016). Observations of five rivers in Ireland; the Erne, Boyne, Blackwater, Brosna and the

Shannon, show that the increase in precipitation results in higher river discharge (Kiely, 1999) (Fig. 5). If similar processes were responsible for high SST/SAT during the Northgrippian and the contribution of the ICC controlled BWT recorded at the core site, we would expect not only a change in temperatures but also a freshening of shelf waters due to the higher contribution of river discharge. The significant correlation between warmer and more saline waters ($r = 0.86$, $p = <.001$, $n = 51$) in our dataset during the Northgrippian suggests however that this is not the case. Finally, a record of past surface water properties from the Celtic Sea (Marret et al., 2004) that lies in the path of the Coastal Current to the south of our core site does not support the hypothesis that Coastal Current waters were warmer during the Northgrippian either. However, we acknowledge that this is a dinocyst record and thus a summer, rather than winter signal (Marret et al., 2004).

5.2. Increased heat advection by the NAC during the Northgrippian (8.2–4.2 ka)

The NAC is an extension of the Gulf Stream originating from the Gulf of Mexico and is predominantly driven by the strength of the westerlies (Bower et al., 2002; Sutton and Allen, 1997). Palaeoceanographic evidence shows that temperatures associated with the Gulf Stream fluctuated by ~1.5 °C over the course of the Holocene, however, a millennial trend or a change in temperature over the Northgrippian – Meghalayan transition, did not occur (Cléroux et al., 2012). Further, records of the eastern limb of the NAC in the Bay of Biscay (550 m, 1472 m and 431 m water depth) provide no evidence for an increase in heat advection during the Northgrippian (Mojtahid et al., 2013; Yannick et al., 2017). Open ocean palaeoceanographic records from the eastern SPG, from sites that lie in the path of the NAC, provide additional evidence for cooler temperatures during the Northgrippian relative to the Meghalayan (Farmer et al., 2008; Risebrobakken et al., 2003, 2011; Staines-Urias et al., 2013; Thornalley et al., 2009). Considering our temperature record demonstrates an opposing trend to palaeoceanographic reconstructions that are influenced by the NAC during the Holocene, it seems unlikely that enhanced heat advection by the NAC towards the eastern boundary of the SPG was responsible for the signal recorded at our core site.

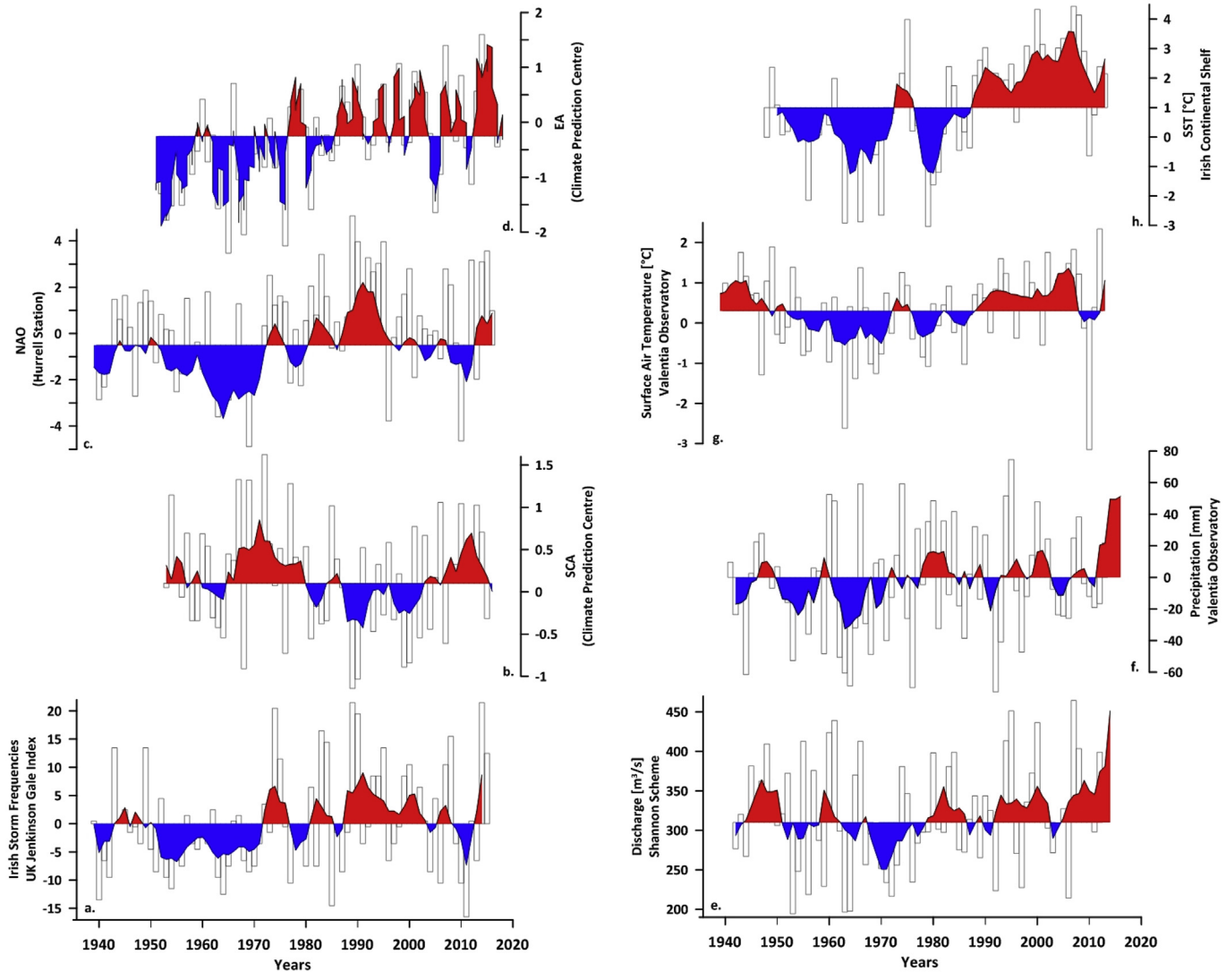

Fig. 5. Modern observations linking local ocean-atmosphere processes for the UK/Irish region. a. Irish storm frequencies (CRU, 2018), *UK Jenkinson Gale Index (Climate Research Unit, University of East Anglia)*, b. SCA Index (NOAA, 2019b), c. NAO Index (Hurrell, 2018), d. EA Index (NOAA, 2019a) e. Averaged DJF discharge from the River Shannon (Ireland), (supplied by ESB from the ESB IOS Hydro Database, *unpublished data*), f. precipitation (MET Éireann, 2018), g. SAT (MET Éireann, 2018), h. SST anomalies, (*Grid: 47.5-57.5 N; 7.5-22.5 W*) *calculated using the Kaplan SST v2 dataset (NOAA)* (Kaplan et al., 1998). Anomalies were calculated using a 30 year reference period 1981–2010.

5.3. Greater influence of Atlantic waters on the Irish Continental Shelf during the Northgrippian (8.2–4.2 ka)

McMahon et al. (1995) suggest that the extent and persistence of the Irish Shelf Front plays a crucial role in the exchange between coastal and oceanic waters including heat and salinity on the Irish Continental Shelf. In a study located in Bantry Bay (south-west Ireland) Raine and McMahon (1998) observed a shift of the Irish Shelf Front in response to the intensity and pathway of the predominant winds. According to Huang et al. (1991) the modern position of the Irish Shelf Front is to the west of our core site (Fig. 1) resulting in relatively cool and fresh conditions east of the front, indicative of a dominant ICC regime. However, a reorganisation of atmospheric conditions within the North Atlantic Region would likely change the predominant wind direction (Pinto and Raible, 2012). Specifically an eastward shift of the Icelandic Low (e.g. Scandinavian pattern, SCA + like conditions) would most likely result in predominant westerlies and thereby move the Irish Shelf Front towards the shore (Raine and McMahon, 1998) and permit a greater proportion of Atlantic waters to reach our core site (Fig. 6). The significant correlation of the 200-year low-pass filter between BWT and $\delta^{18}O_{sw}$ ($r = 0.86$, $p = <.001$, $n = 51$) during the regional climate optimum validates the argument of in-phase variability during this period, supporting the hypothesis of a greater intrusion of Atlantic waters at our core.

5.4. Linking local changes to large-scale ocean-atmospheric variability in North Atlantic Region

The most recent analogues for an eastward shift of the Icelandic Low (SCA + like conditions) occurred during the 1920s–1940s and early 2000s (Bengtsson et al., 2004; Moore et al., 2013; Overland et al., 2004; Overland and Wang, 2005). During both periods, pronounced warming of the climate system, particularly at high northern latitudes (Bengtsson et al., 2004) coincided with significant sea-ice decline, warm SST and SAT anomalies in the Barents Sea and SPG Region (Bengtsson et al., 2004; Smedsrud et al., 2013) and within the instrumental record the largest reduction in Greenland Ice-Sheet mass (Andresen et al., 2012). Here we concentrate on the period between ~1920 and 1940.

The leading hypotheses for the 1920–1940s climate anomaly include the combination of anthropogenic effects, increased solar radiation, reduced volcanic activity, and natural climate variability (e.g. El Niño-Southern Oscillation, AMO and Pacific Decadal Oscillation (PDO)) (Bengtsson et al., 2004; Hegerl et al., 2018; Overland et al., 2004; Tokinaga et al., 2017). A review paper by Smedsrud et al. (2013) suggests the climate anomaly was most likely forced by the ocean through increased advection of warm Atlantic waters into the Barents Sea thereby reducing sea-ice extent. Moreover, the importance of increased SST in driving atmospheric variations during this period is emphasised in a coupled ocean–atmosphere model by Tokinaga et al. (2017). Specifically in this study, authors associate a warm phase of the PDO with AMO + like conditions to explain the warmth of the 1920–1940s. However the attribution of the PDO to the 1920–1940s climate anomaly is still debated (Hegerl et al., 2018). For more information on this topic the reader is referred to a recent review paper by Hegerl et al. (2018) and references therein for further discussion.

The impact of the eastward shift of the Icelandic Low on SPG dynamics during the 1920–40 period was important. First, the shift diminished the atmospheric pressure gradient between the Greenland High and Icelandic Low, resulting in slackened winds along the East Greenland coast, which in turn weakened the East Greenland Current (EGC) (Blindheim and Malmberg, 2005). This reduction of the EGC affected the freshwater balance and increased SST in the Irminger Sea Basin. As a result the warmer SST reduced

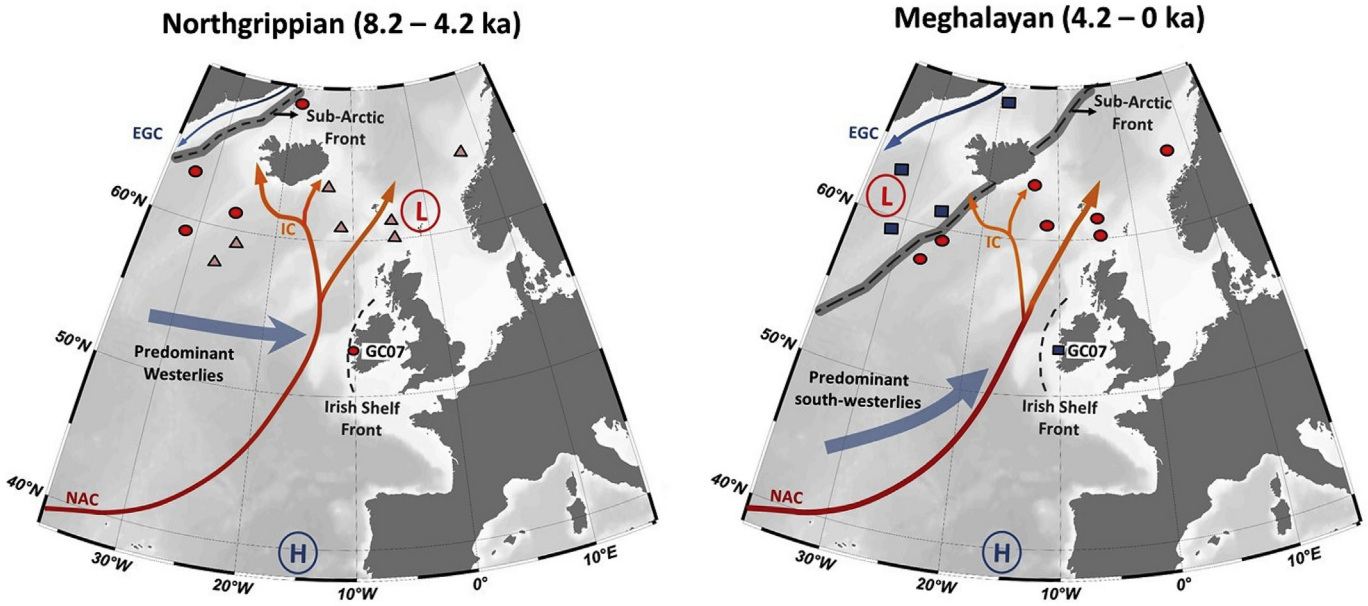

Fig. 6. Northgrippian and Meghalayan ocean-atmosphere conditions: Left panel shows the impact of an eastward shift of Icelandic Low to the Southern Nordic Seas on the Northeast Atlantic i.e. reduced influence of East Greenland Current (EGC) to the subpolar North Atlantic, increased influence of Irminger Current (IC) North of Iceland, a north-west shift of the Sub-Arctic Front to the North and west of Iceland during the Northgrippian. The predominant westerlies push the Irish Shelf Front to the east relative to GC07. Right panel shows the impact of a westward shift of Icelandic Low to its modern (e.g. NAO) position in the Irminger Sea Basin, resulting in increased EGC influence to the subpolar North Atlantic, decreased influence of IC North of Iceland, south-east shift of the Sub-Arctic Front, westerlies are predominately from the south-west resulting in a westward positioned Irish Shelf Front, indicative of modern NAO − like conditions. The squares/circles/triangles represent published studies from the North Atlantic. Red circles indicate warm conditions; blue squares indicate cold conditions and pink triangles indicate cool conditions. Please consult the supplementary section for a full list of references. (For interpretation of the references to colour in this figure legend, the reader is referred to the Web version of this article.)

the density gradient across the gyre (Muller et al., 2015), weakened SPG circulation and increased the influence of the Irminger Current to the north and west of Iceland, all contributing to extremely warm AMO + like conditions (Trenberth and Shea, 2006). These increased temperatures during the 1920–1940s also led to enhanced melting of marine-terminating glaciers on the East Greenland Shelf (Andresen et al., 2012). Finally, observations by Allan et al. (2009) show that the 1920–40 period coincided with peak storminess over the British Isles.

Taking both observational evidence and model results into account, the climatic response to an eastward shift of the Icelandic Low (SCA + like conditions) thus are (1) increased SST in the Irminger Sea Basin and the Greenland Sea, (2) significantly reduced sea-ice extent in the Barents Sea, (3) increased melting of marine-terminating glaciers on the eastern margin of the Greenland Shelf and (4) increased storminess for the Ireland/UK region. Assuming the ocean-atmosphere conditions during this period are an appropriate analogue for the Northgrippian, we would expect to see similar trends in palaeoreconstructions.

The significantly warmer and saltier SST in the Irminger Sea Basin (Came et al., 2007; Jennings et al., 2002, 2011; Morley et al., 2014; Moros et al., 2012), compared to cooler SST in the eastern SPG during the Northgrippian (Farmer et al., 2008; Risebrobakken et al., 2003, 2011; Thornalley et al., 2009) appear to support the hypothesis of an eastward shift of the Icelandic Low to the Southern Nordic Seas (Fig. 7). Given the evidence for the enhanced contribution of warm Irminger Current waters on the eastern margin of the Greenland Shelf and the high-sensitivity of marine-terminating glaciers to warmer Atlantic waters we speculate that this shift in atmospheric circulation would also have enhanced melting of (any remaining) marine-terminating glaciers during the Northgrippian. However, this is a tentative suggestion as unlike the 1930s, records for the Northgrippian from the East Greenland margin provide no evidence of increased calving of the Greenland Ice-Sheet (Jennings et al., 2002, 2011; Risebrobakken et al., 2011). This is likely due to the absence of sustained marine-terminating glaciers on the East Greenland margin during the warmer than present Northgrippian (Larsen et al., 2015). Nonetheless, this has implications for future climate change scenarios, as a sustained presence of the Irminger Current on the East Greenland Shelf would accelerate the melting of marine-terminating glaciers and thereby freshen surface waters in the western subpolar gyre.

Further support for an eastward shift of the Icelandic Low to the Southern Nordic Seas can be drawn from a study by Olafsdottir et al. (2010) who provide evidence of increased storminess after ~4 ka at a site located south-west of Iceland, indicative of a more proximal position of the Icelandic Low to Iceland during the Meghalayan. Significant glacier growth in Scandinavia, most likely driven by increased westerly circulation, after the Northgrippian – Meghalayan transition (Bakke et al., 2008, 2010; Balascio and Bradley, 2012; Nesje, 2009) can also be explained by a shift from SCA + like conditions towards more modern NAO – like conditions. Finally, most sea-ice reconstructions and modelling data provided by the Paleoclimate Modelling Intercomparison Project (PMIP) phase 1–3 (Zhang et al., 2010) provide evidence for a substantial decrease in sea-ice extent during the Greenlandian – Northgrippian stages compared to that of pre-industrial conditions (Stranne et al., 2014). Taking into account the available palaeoceanographic and modelling evidence from the Northgrippian, the data thus appears to support the hypothesis of an eastward shift of the Icelandic Low (SCA – like conditions) during this period.

The warm event centred at 2.4 ± 0.2 ka in our dataset is also recorded in other palaeoceanographic records across the North Atlantic Region (Morley et al., 2014; Moros et al., 2012; Perner et al., 2018) and is often referred to as the Roman Warm Period (RWP). This period is interesting as maximum salinity values coincide with

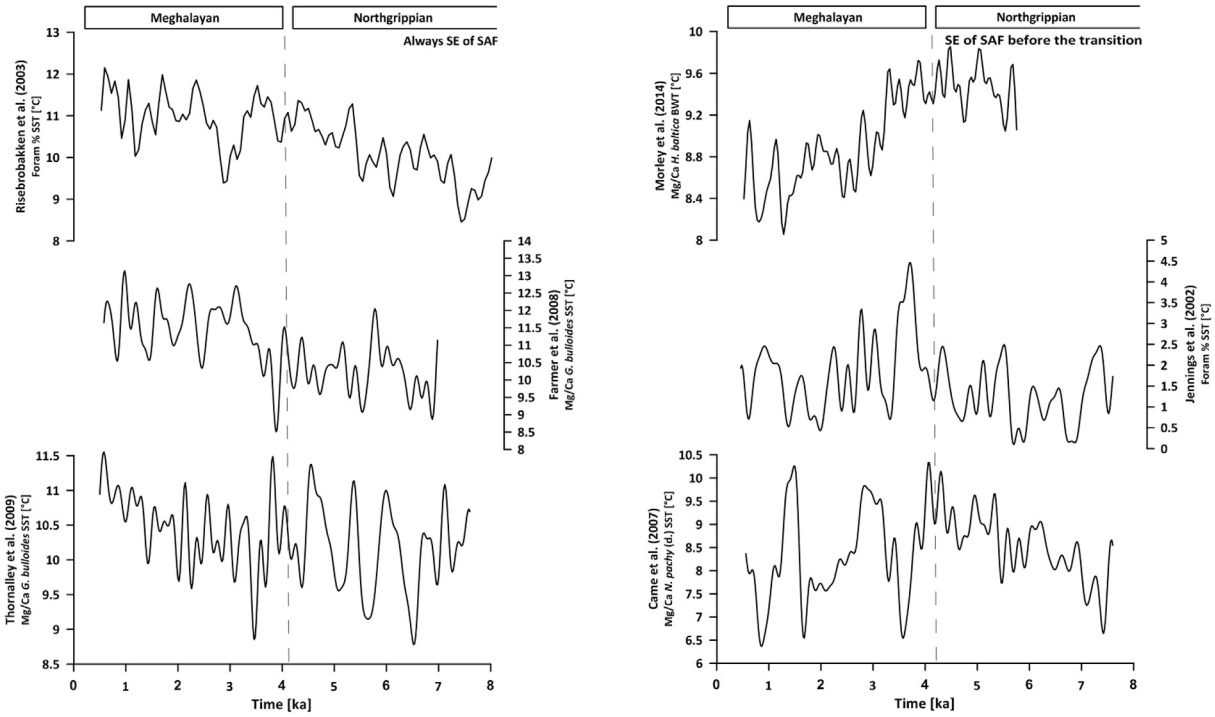

Fig. 7. Comparison of records from the North Atlantic Region. All time series are shown with a 200-year low-pass filter. Records always south-east of the Sub-Arctic Front – left panel (Farmer et al., 2008; Risebrobakken et al., 2003; Thornalley et al., 2009) exhibit a long-term warming trend over Holocene Epoch. Records to the south-east of the Sub-Arctic Front during the Northgrippian (8.2–4.2 ka) and to the northwest of the Sub-Arctic Front during the Meghalayan (4.2–0 ka) - right panel (Came et al., 2007; Jennings et al., 2002; Morley et al., 2014) exhibit a general warming until the transition and thereafter a cooling trend.

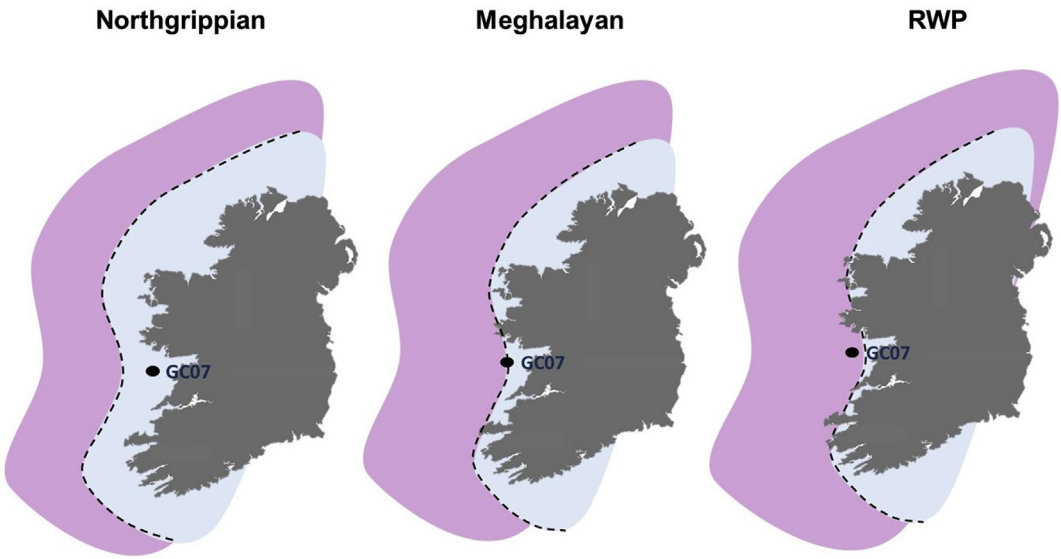

Fig. 8. Schematic representation of differing oceanic conditions on the Irish Continental Shelf during the Northgrippian, the Meghalayan and the RWP. Blue (light grey in greyscale) represents cool and low salinity ICC waters. Pink (dark grey in greyscale) represents warm and saline Atlantic waters. Dashed line indicating the position of the Irish Shelf Front. The position of the front is determined by the intensity and pathway of the predominant winds. Northgrippian conditions indicative of mixed ICC and Atlantic waters at our core site. Meghalayan conditions indicative of primarily ICC waters at our core site. RWP conditions indicative of primarily Atlantic waters at our core site. (For interpretation of the references to colour in this figure legend, the reader is referred to the Web version of this article.)

increased BWT. Unlike the Northgrippian however, the background climate in the North Atlantic Region differs from SCA − like conditions. Most importantly, long-term records of atmospheric (westerly circulation) influenced glaciers in western Scandinavia (Wanner et al., 2008) demonstrate stability or expansion during this period (Bakke et al., 2008, 2010; Matthews and Dresser, 2008; Nesje, 2009), which is contrary to the dry and warm conditions that characterised Scandinavian climate during the Northgrippian and the modern SCA + mode. The NAO dipole is equally at odds with local and regional palaeobservations for the RWP. This is because a strong NAO (+) pattern (necessary to describe our local observations) would imply colder SST (or AMO -) in the centre of the SPG (Johnson and Gruber, 2007), which disagrees with several palaeoceanographic reconstructions that provide evidence for warm SST at the centre of the SPG at that time (Farmer et al., 2008; Morley et al., 2014; Moros et al., 2012; Perner et al., 2018).

Alternatively, a southward shift of the low-pressure system to the west of Ireland as observed during years dominated by a positive EA (EA +) pattern may unite palaeobservations for the RWP. Locally, the proximity of the low-pressure systems to the west coast of Ireland would have enhanced local westerly wind stress and thereby increased the contribution of Atlantic waters at the core site by moving the Irish Shelf Front towards the shore (Fig. 8), while the eastward shift of the low would have reduced heat loss and led to warmer SST over the Irminger Sea Basin. Further afield, observational records highlight that the southward displacement of the dominant low during EA + years enhances precipitation in the Iberian Peninsula (Rodriguez-Puebla et al., 1998). Interestingly several palaeo-records from the Iberian Peninsula highlight the RWP as an exceptionally wet period (Martín-Puertas et al., 2009).

6. Conclusions

Here we tested the hypothesis that warmer than present climates in the North Atlantic Region may lead to an eastward shift of the Icelandic Low to the Southern Nordic Seas. Our results and analysis suggests that a spatial reorganisation of the Icelandic Low changed the predominant wind direction of the westerlies during the regional climate optimum (4–5 ka). As a result, the westerlies pushed the Irish Shelf Front towards the shore, allowing a greater intrusion of Atlantic waters (warm and saline conditions) onto the Irish Continental Shelf. We postulate that a SCA + like atmospheric organisation within the North Atlantic Region is the most likely explanation for the shift of prevailing winds from south-westerly to predominant westerly winds that could account for the shift of the Irish Shelf Front. Moreover, SCA + like conditions are also consistent with palaeoceanographic and terrestrial palaeoclimate records from the North Atlantic Region during the Northgrippian. Assuming the Northgrippian is a useful analogue for future atmospheric changes over the North Atlantic Region an eastward shift of the Icelandic Low is likely to result in increased magnitude and frequency of storm events for the UK and Ireland due to their proximity to the centre of low-pressure system. This atmospheric configuration is also likely to increase the northward influence of the Irminger Current and thereby enhance the melting of marine-terminating glaciers on the eastern margin of the East Greenland Shelf as observed during the 1930s and early 2000s (Andresen et al., 2012). Our findings also highlights the importance of the RWP (~2.4 ka) and a possible link to EA + like conditions. Limited research has been carried out on this type of configuration and its impact for the UK and Ireland region, however it is likely this pattern would also result in increased magnitude and frequency of storm events for the region due to the proximity of the low-pressure centre.

Palaeoreconstructions are crucial to better understand ocean-atmospheric circulation changes operating on multidecadal to centennial timescales. By situating our regional record into an extra-regional to hemispheric context we were able to evaluate the ocean-atmosphere dynamics of the North Atlantic Region that operated during the Holocene. Our contribution provides an improved understanding of the complex ocean-atmosphere-sea-ice system that operated Northgrippian – Meghalayan transition within the North Atlantic, which is important if we are to manage, protect and adapt against future high-impact climate events in a warming world.

Declaration of competing interest

We confirm there are no conflicts of interest with this submission and all authors agree to this submission.

Acknowledgements

This project was partially funded by the Irish Research Council New Foundations scheme. The collection of the core GC07 was funded by a Grant-in-Aid Application for the National Research Vessels 2015 Ship-Time Programme funded by the Marine Institute and awarded to AM. The authors wish to thank the captains and crew of the *R.V. Celtic Voyager* for their part in successful sample retrieval, as well as the scientific parties aboard. We would also like to acknowledge the Marine Institute Networking and Travel Grant and express our gratitude to The Irish Quaternary Association (IQUA) and the 14CHRONO Centre at Queen's University Belfast for providing two radiocarbon dates through the Bill Watts 14 Chrono Award. MC is the recipient of the Galway Doctoral Research Scholarship awarded by the National University of Ireland, Galway. Finally, we would like to thank Antje Volker and two anonymous reviewers for their helpful comments and suggestions, which greatly improved the manuscript. All data used in this study are available online through the Pangaea website, https://doi.org/10.1594/PANGAEA.907706.

Appendix A. Supplementary data

Supplementary data to this article can be found online at https://doi.org/10.1016/j.quascirev.2019.106004.

References

Allan, R., Tett, S., Alexander, L., 2009. Fluctuations in autumn–winter severe storms over the British Isles: 1920 to present. Int. J. Climatol. 29, 357–371. https://doi.org/10.1002/joc.1765.

Anderson, D.M., 2001. Attenuation of millennial-scale events by bioturbation in marine sediments. Paleoceanogr. Paleoclimatol. 16, 352–357. https://doi.org/10.1029/2000PA000530.

Andresen, C.S., Straneo, F., Ribergaard, M.H., Bjork, A.A., Andersen, T.J., Kuijpers, A., Norgaard-Pedersen, N., Kjaer, K.H., Schjoth, F., Weckstrom, K., Ahlstrom, A.P., 2012. Rapid response of Helheim Glacier in Greenland to climate variability over the past century. Nat. Geosci. 5, 37–41. https://doi.org/10.1038/Ngeo1349.

Ascough, P., Cook, G., Dugmore, A., 2009. North Atlantic marine 14C reservoir effects: implications for late-Holocene chronological studies. Quat. Geochronol. 4, 171–180.

Austin, W.E.N., Cage, A.G., Scourse, J.D., 2006. Mid-latitude shelf seas: a NW European perspective on the seasonal dynamics of temperature, salinity and oxygen isotopes. Holocene 16, 937–947. https://doi.org/10.1177/0959683606hl985rp.

Bakke, J., Lie, Ø., Dahl, S.O., Nesje, A., Bjune, A.E., 2008. Strength and spatial patterns of the Holocene wintertime westerlies in the NE Atlantic region. Glob. Planet. Chang. 60, 28–41. https://doi.org/10.1016/j.gloplacha.2006.07.030.

Bakke, J., Dahl, S.O., Paasche, Ø., Riis Simonsen, J., Kvisvik, B., Bakke, K., Nesje, A., 2010. A complete record of Holocene glacier variability at Austre Okstindbreen, northern Norway: an integrated approach. Quat. Sci. Rev. 29, 1246–1262. https://doi.org/10.1016/j.quascirev.2010.02.012.

Balascio, N.L., Bradley, R.S., 2012. Evaluating Holocene climate change in northern Norway using sediment records from two contrasting lake systems. J. Paleolimnol. 48, 259–273. https://doi.org/10.1007/s10933-012-9604-7.

Bamberg, A., Rosenthal, Y., Paul, A., Heslop, D., Mulitza, S., Rühlemann, C., Schulz, M., 2010. Reduced North Atlantic central water formation in response to early Holocene ice-sheet melting. Geophys. Res. Lett. 37, L17705. https://doi.org/10.1029/2010GL043878.

Barnston, A.G., Livezey, R.E., 1987. Classification, seasonality and persistence of low-frequency atmospheric circulation patterns. Mon. Weather Rev. 115, 1083–1126. https://doi.org/10.1175/1520-0493(1987)115<1083:Csapol>2.0.Co;2.

Bemis, B.E., Spero, H.J., Bijma, J., Lea, D.W., 1998. Reevaluation of the oxygen isotopic composition of planktonic foraminifera: experimental results and revised paleotemperature equations. Paleoceanography 13, 150–160.

Bengtsson, L., Semenov, V.A., Johannessen, O.M., 2004. The early twentieth-century warming in the arctic—a possible mechanism. J. Clim. 17, 4045–4057. https://doi.org/10.1175/1520-0442(2004)017<4045:tetwit>2.0.co;2.

Bjerknes, J., 1964. Atlantic air-sea interaction. Adv. Geophys. 10, 1–82.

Blaauw, M., Christen, J.A., 2013. Bacon Manual e v2. 2. Blaauw, M., Wohlfarth, B., Christen, JA, Ampel, L., Veres, D., Hughen, KA, Preusser, F., et al.(2010),—Were Last Glacial Climate Events Simultaneous between Greenland and France, 387-394.

Blindheim, J., Malmberg, S.A., 2005. The Mean Sea Level Pressure Gradient across the Denmark Strait as an Indicator of Conditions in the North Icelandic Irminger Current, the Nordic Seas: an Integrated Perspective Oceanography, Climatology, Biogeochemistry, and Modeling. AGU, Washington, DC, pp. 65–71.

Bower, A., Le Cann, B., Rossby, T., Zenk, W., Gould, J., Speer, K., Richardson, P., Prater, M., Zhang, H.-M., 2002. Directly measured mid-depth circulation in the northeastern North Atlantic Ocean. Nature 419, 603.

Bueh, C., Nakamura, H., 2007. Scandinavian pattern and its climatic impact. Quart. J. Roy. Meteorol. Soc 133, 2117–2131. https://doi.org/10.1002/qj.173.

Came, R.E., Oppo, D.W., McManus, J.F., 2007. Amplitude and timing of temperature and salinity variability in the subpolar North Atlantic over the past 10 k.y. Geology 35, 315–318. https://doi.org/10.1130/g23455a.1.

Charpentier Ljungqvist, F., 2011. The spatio-temporal pattern of the mid-Holocene thermal maximum. Geogr.–Sb. CGS 116, 91–110.

Cléroux, C., Debret, M., Cortijo, E., Duplessy, J.C., Dewilde, F., Reijmer, J., Massei, N., 2012. High-resolution sea surface reconstructions off Cape Hatteras over the last 10 ka. Paleoceanogr. Paleoclimatol. 27 https://doi.org/10.1029/2011PA002184.

Comas-Bru, L., McDermott, F., 2014. Impacts of the EA and SCA patterns on the European twentieth century NAO–winter climate relationship. Quart. J. Roy. Meteorol. Soc 140, 354–363. https://doi.org/10.1002/qj.2158.

CRU, 2018. UK Jenkinson Gale Index.

Cunningham, L.K., Austin, W.E., Knudsen, K.L., Eiríksson, J., Scourse, J.D., Wanamaker Jr., A.D., Butler, P.G., Cage, A.G., Richter, T., Husum, K., 2013. Reconstructions of surface ocean conditions from the northeast Atlantic and Nordic seas during the last millennium. Holocene 23, 921–935.

Curry, R.G., McCartney, M.S., 2001. Ocean gyre circulation changes associated with the North Atlantic oscillation. J. Phys. Oceanogr. 31, 3374–3400. https://doi.org/10.1175/1520-0485(2001)031<3374:Ogccaw>2.0.Co;2.

Davis, B., Brewer, S., 2009. Orbital forcing and role of the latitudinal insolation/temperature gradient. Clim. Dyn. 32, 143–165. https://doi.org/10.1007/s00382-008-0480-9.

Dickson, B., Yashayaev, I., Meincke, J., Turrell, B., Dye, S., Holfort, J., 2002. Rapid freshening of the deep North Atlantic Ocean over the past four decades. Nature 416, 832–837.

Fairbanks, R.G., 1989. A 17,000-year glacio-eustatic sea-level record - influence of glacial melting rates on the younger dryas event and deep-ocean circulation. Nature 342, 637–642. https://doi.org/10.1038/342637a0.

Farmer, E.J., Chapman, M.R., Andrews, J.E., 2008. Centennial-scale Holocene North Atlantic surface temperatures from Mg/Ca ratios in Globigerina bulloides. Geochem. Geophys. Geosyst. 9 https://doi.org/10.1029/2008GC002199.

Fernand, L., Nolan, G., Raine, R., Chambers, C., Dye, S., White, M., Brown, J., 2006. The Irish coastal current: a seasonal jet-like circulation. Cont. Shelf Res. 26, 1775–1793.

Feser, F., Barcikowska, M., Krueger, O., Schenk, F., Weisse, R., Xia, L., 2014. Storminess over The north atlantic and northwestern europe—a review. Quart. J. Roy. Meteorol. Soc. https://doi.org/10.1002/qj.2364 n/a-n/a.

Friedman, I., O'Neil, J.R., 1977. Data of Geochemistry: Compilation of Stable Isotope Fractionation Factors of Geochemical Interest. US Government Printing Office.

Giraudeau, J., Grelaud, M., Solignac, S., Andrews, J.T., Moros, M., Jansen, E., 2010. Millennial-scale variability in Atlantic water advection to the Nordic Seas derived from Holocene coccolith concentration records. Quat. Sci. Rev. 29, 1276–1287. https://doi.org/10.1016/j.quascirev.2010.02.014.

Gulev, S.K., Latif, M., Keenlyside, N., Park, W., Koltermann, K.P., 2013. North Atlantic Ocean control on surface heat flux on multidecadal timescales. Nature 499, 464–467. https://doi.org/10.1038/nature12268.

Hall, R., Erdelyi, R., Hanna, E., Jones, J.M., Scaife, A.A., 2015. Drivers of North atlantic polar front jet stream variability. Int. J. Climatol. 35, 1697–1720. https://doi.org/10.1002/joc.4121.

Hátún, H., Sandø, A.B., Drange, H., Hansen, B., Valdimarsson, H., 2005. Influence of the Atlantic subpolar gyre on the thermohaline circulation. Science 309, 1841–1844.

Hegerl, G.C., Bronnimann, S., Schurer, A., Cowan, T., 2018. The early 20th century warming: anomalies, causes, and consequences. Wiley Interdiscip. Rev. Clim. Change 9, e522. https://doi.org/10.1002/wcc.522.

Hill, A., Brown, J., Fernand, L., Holt, J., Horsburgh, K., Proctor, R., Raine, R., Turrell, W., 2008. Thermohaline circulation of shallow tidal seas. Geophys. Res. Lett. 35.

Holliday, N., 2003. Air-sea interaction and circulation changes in the northeast Atlantic. J. Geophys. Res.: Oceans 108.

Huang, W.G., Cracknell, A.P., Vaughan, R.A., Davies, P.A., 1991. A satellite and field View of the Irish shelf front. Cont. Shelf Res. 11, 543–562. https://doi.org/10.1016/0278-4343(91)90010-4.

Huntingford, C., Marsh, T., Scaife, A.A., Kendon, E.J., Hannaford, J., Kay, A.L., Lockwood, M., Prudhomme, C., Reynard, N.S., Parry, S., Lowe, J.A., Screen, J.A., Ward, H.C., Roberts, M., Stott, P.A., Bell, V.A., Bailey, M., Jenkins, A., Legg, T., Otto, F.E.L., Massey, N., Schaller, N., Slingo, J., Allen, M.R., 2014. Potential influences on the United Kingdom's floods of winter 2013/14. Nat. Clim. Chang. 4, 769–777. https://doi.org/10.1038/Nclimate2314.

Hurrell, J.W., 1995. Decadal trends in the north atlantic oscillation: regional temperatures and precipitation. Science 269, 676–679. https://doi.org/10.1126/science.269.5224.676.

Hurrell, J.W., Kushnir, Y., Ottersen, G., Visbeck, M., 2003. The North Atlantic Oscillation. American Geophysical Union, Washington.

Hurrell, J., 2018. National Center for Atmospheric Research Staff. In: The Climate Data Guide: Hurrell North Atlantic Oscillation (NAO) Index (station-based). Retrieved from. https://climatedataguide.ucar.edu/climate-data/hurrell-north-atlantic-oscillation-nao-index-station-based.
Jennings, A.E., Knudsen, K.L., Hald, M., Hansen, C.V., Andrews, J.T., 2002. A mid-Holocene shift in Arctic sea-ice variability on the East Greenland Shelf. Holocene 12, 49–58. https://doi.org/10.1191/0959683602hl519rp.
Jennings, A., Andrews, J., Wilson, L., 2011. Holocene environmental evolution of the SE Greenland shelf north and south of the Denmark strait: Irminger and East Greenland current interactions. Quat. Sci. Rev. 30, 980–998. https://doi.org/10.1016/j.quascirev.2011.01.016.
Johnson, G.C., Gruber, N., 2007. Decadal water mass variations along 20°W in the northeastern Atlantic ocean. Prog. Oceanogr. 73, 277–295.
Kaplan, A., Cane, M.A., Kushnir, Y., Clement, A.C., Blumenthal, M.B., Rajagopalan, B., 1998. Analyses of global sea surface temperature 1856–1991. J. Geophys. Res.: Oceans 103, 18567–18589. https://doi.org/10.1029/97JC01736.
Kiely, G., 1999. Climate change in Ireland from precipitation and streamflow observations. Adv. Water Resour. 23, 141–151. https://doi.org/10.1016/S0309-1708(99)00018-4.
Knight, J.R., Allan, R.J., Folland, C.K., Vellinga, M., Mann, M.E., 2005. A signature of persistent natural thermohaline circulation cycles in observed climate. Geophys. Res. Lett. 32, L20708. https://doi.org/10.1029/2005gl024233.
Knight, J.R., Folland, C.K., Scaife, A.A., 2006. Climate impacts of the Atlantic multidecadal oscillation. Geophys. Res. Lett. 33.
Kutzbach, J.E., Webb III, T., 1993. Conceptual basis for understanding Late-Quaternary climates. In: Wright Jr., H.E., Kutzbach, J.E., Webb III, T., Ruddiman, W.F., Street-Perrott, F.A., Bartlein, P.J. (Eds.), Global Climates since the Last Glacial Maximum. University of Minnesota Press, pp. 5–11.
Laepple, T., Lohmann, G., 2009. Seasonal cycle as template for climate variability on astronomical timescales. Paleoceanography 24.
Larsen, N.K., Kjaer, K.H., Lecavalier, B., Bjork, A.A., Colding, S., Huybrechts, P., Jakobsen, K.E., Kjeldsen, K.K., Knudsen, K.L., Odgaard, B.V., Olsen, J., 2015. The response of the southern Greenland ice sheet to the Holocene thermal maximum. Geology 43, 291–294. https://doi.org/10.1130/G36476.1.
Le Mezo, P., Lefort, S., Seferian, R., Aumont, O., Maury, O., Murtugudde, R., Bopp, L., 2016. Natural variability of marine ecosystems inferred from a coupled climate to ecosystem simulation. J. Mar. Syst. 153, 55–66. https://doi.org/10.1016/j.jmarsys.2015.09.004.
Leduc, G., Schneider, R., Kim, J.-H., Lohmann, G., 2010. Holocene and Eemian sea surface temperature trends as revealed by alkenone and Mg/Ca paleothermometry. Quat. Sci. Rev. 29, 989–1004.
Liu, Z., Zhu, J., Rosenthal, Y., Zhang, X., Otto-Bliesner, B.L., Timmermann, A., Smith, R.S., Lohmann, G., Zheng, W., Timm, O.E., 2014. The Holocene temperature conundrum. Proc. Natl. Acad. Sci. 111, E3501–E3505.
Lynch-Stieglitz, J., Curry, W.B., Slowey, N., 1999. A geostrophic transport estimate for the Florida Current from the oxygen isotope composition of benthic foraminifera. Paleoceanography 14, 360–373.
Marchitto, T., Curry, W., Lynch-Stieglitz, J., Bryan, S., Cobb, K., Lund, D., 2014. Improved oxygen isotope temperature calibrations for cosmopolitan benthic foraminifera. Geochem. Cosmochim. Acta 130, 1–11.
Marcott, S.A., Shakun, J.D., Clark, P.U., Mix, A.C., 2013. A reconstruction of regional and global temperature for the past 11,300 years. Science 339, 1198–1201. https://doi.org/10.1126/science.1228026.
Marret, F., Scourse, J., Austin, W., 2004. Holocene shelf-sea seasonal stratification dynamics: a dinoflagellate cyst record from the Celtic Sea, NW European shelf. Holocene 14, 689–696. https://doi.org/10.1191/0959683604hl747rp.
Martin, J., Lusher, A., Thompson, R.C., Morley, A., 2017. The deposition and accumulation of microplastics in marine sediments and bottom water from the Irish continental shelf. Sci. Rep. 7, 10772. https://doi.org/10.1038/s41598-017-11079-2.
Martín-Puertas, C., Valero-Garcés, B.L., Brauer, A., Mata, M.P., Delgado-Huertas, A., Dulski, P., 2009. The Iberian–Roman humid period (2600–1600 cal yr BP) in the Zoñar lake varve record (andalucía, southern Spain). Quat. Res. 71, 108–120. https://doi.org/10.1016/j.yqres.2008.10.004.
Matthews, J.A., Dresser, P.Q., 2008. Holocene glacier variation chronology of the Smørstabbtindan massif, Jotunheimen, southern Norway, and the recognition of century-to millennial-scale European Neoglacial events. Holocene 18, 181–201. https://doi.org/10.1177/0959683607085608.
Matthews, T., Mullan, D., Wilby, R.L., Broderick, C., Murphy, C., 2016. Past and future climate change in the context of memorable seasonal extremes. Clim. Risk Manag. 11, 37–52. https://doi.org/10.1016/j.crm.2016.01.004.
McMahon, T., Raine, R., Titov, O., Boychuk, S., 1995. Some oceanographic features of northeastern atlantic waters west of Ireland. ICES J. Mar. Sci. 52, 221–232. https://doi.org/10.1016/1054-3139(95)80037-9.
MET Éireann, 2018. Historical Data.
Mojtahid, M., Jorissen, F., Garcia, J., Schiebel, R., Michel, E., Eynaud, F., Gillet, H., Cremer, M., Ferreiro, P.D., Siccha, M., 2013. High resolution Holocene record in the southeastern Bay of Biscay: global versus regional climate signals. Palaeogeogr. Palaeoclimatol. Palaeoecol. 377, 28–44.
Moore, G., Renfrew, I., 2012. Cold european winters: interplay between the NAO and the east atlantic mode. Atmos. Sci. Lett. 13, 1–8.
Moore, G.W.K., Pickart, R.S., Renfrew, I.A., 2011. Complexities in the climate of the subpolar North Atlantic: a case study from the winter of 2007. Quart. J. Roy. Meteorol. Soc 137, 757–767. https://doi.org/10.1002/qj.778.
Moore, G.W.K., Renfrew, I.A., Pickart, R.S., 2013. Multidecadal mobility of The north atlantic oscillation. J. Clim. 26, 2453–2466. https://doi.org/10.1175/Jcli-D-12-00023.1.
Morley, A., Rosenthal, Y., Demenocal, P., 2014. Ocean-atmosphere climate shift during the mid-to-late Holocene transition. Earth Planet. Sci. Lett. 388, 18–26. https://doi.org/10.1016/j.epsl.2013.11.039.
Moros, M., Jansen, E., Oppo, D.W., Giraudeau, J., Kuijpers, A., 2012. Reconstruction of the late-holocene changes in the sub-arctic front position at the reykjanes ridge, North Atlantic. Holocene 22, 877–886. https://doi.org/10.1177/0959683611434224.
Morrill, J.C., Bales, R.C., Conklin, M.H., 2005. Estimating stream temperature from air temperature: implications for future water quality. J. Environ. Eng. 131, 139–146. https://doi.org/10.1061/(Asce)0733-9372(2005)131:1(139).
Müller, J., Werner, K., Stein, R., Fahl, K., Moros, M., Jansen, E., 2012. Holocene cooling culminates in sea ice oscillations in Fram Strait. Quat. Sci. Rev. 47, 1–14.
Muller, W.A., Matei, D., Bersch, M., Jungclaus, J.H., Haak, H., Lohmann, K., Compo, G.P., Sardeshmukh, P.D., Marotzke, J., 2015. A twentieth-century reanalysis forced ocean model to reconstruct the North Atlantic climate variation during the 1920s. Clim. Dyn. 44, 1935–1955. https://doi.org/10.1007/s00382-014-2267-5.
Nesje, A., 2009. Latest pleistocene and Holocene alpine glacier fluctuations in Scandinavia. Quat. Sci. Rev. 28, 2119–2136.
NOAA, C.P.C., 2019a. East Atlantic (EA).
NOAA, C.P.C., 2019b. Scandinavia (SCAND).
Nolan, G., Lyons, K., 2006. Ocean Climate Variability on the Western Irish Shelf, an Emerging Time Series, vol. 100. International Council for the Exploration of the Sea (CM papers and reports), CM, p. 28.
Olafsdottir, S., Jennings, A.E., Geirsdottir, A., Andrews, J., Miller, G.H., 2010. Holocene variability of the North Atlantic Irminger current on the south- and northwest shelf of Iceland. Mar. Micropaleontol. 77, 101–118. https://doi.org/10.1016/j.marmicro.2010.08.002.
Osborn, T.J., 2006. Recent variations in the winter North Atlantic oscillation. Weather 61, 353–355.
Overland, J.E., Wang, M.Y., 2005. The third Arctic climate pattern: 1930s and early 2000s. Geophys. Res. Lett. 32, L23808 https://doi.org/10.1029/2005gl024254.
Overland, J.E., Spillane, M.C., Percival, D.B., Wang, M.Y., Mofjeld, H.O., 2004. Seasonal and regional variation of pan-Arctic surface air temperature over the instrumental record. J. Clim. 17, 3263–3282. https://doi.org/10.1175/1520-0442(2004)017<3263:Sarvop>2.0.Co;2.
Peings, Y., Magnusdottir, G., 2014. Forcing of the wintertime atmospheric circulation by the multidecadal fluctuations of the North Atlantic ocean. Environ. Res. Lett. 9, 034018 https://doi.org/10.1088/1748-9326/9/3/034018.
Perner, K., Moros, M., Jansen, E., Kuijpers, A., Troelstra, S.R., Prins, M.A., 2018. Subarctic Front migration at the Reykjanes Ridge during the mid-to late Holocene: evidence from planktic foraminifera. Boreas 47, 175–188. https://doi.org/10.1111/bor.12263.
Pingree, R.D., Lecann, B., 1989. Celtic and armorican slope and shelf residual currents. Prog. Oceanogr. 23, 303–338. https://doi.org/10.1016/0079-6611(89)90003-7.
Pinto, J.G., Raible, C.C., 2012. Past and recent changes in the North Atlantic oscillation. Wires Clim. Change 3, 79–90. https://doi.org/10.1002/wcc.150.
Pinto, J.G., Zacharias, S., Fink, A.H., Leckebusch, G.C., Ulbrich, U., 2009. Factors contributing to the development of extreme North Atlantic cyclones and their relationship with the NAO. Clim. Dyn. 32, 711–737. https://doi.org/10.1007/s00382-008-0396-4.
Raine, R., 2014. A review of the biophysical interactions relevant to the promotion of HABs in stratified systems: the case study of Ireland. Deep-Sea Res. Pt Ii 101, 21–31. https://doi.org/10.1016/j.dsr2.2013.06.021.
Raine, R., McMahon, T., 1998. Physical dynamics on the continental shelf off southwestern Ireland and their influence on coastal phytoplankton blooms. Cont. Shelf Res. 18, 883. https://doi.org/10.1016/S0278-4343(98)00017-X.
Raine, R., McMahon, T., Roden, C., 1993. A review of the summer phytoplankton distribution in Irish coastal waters: a biogeography related to physical oceanography. Biogeography of Ireland: past, present, and future. Occ. Publ. Ireland Biogeogr. Soc. 2, 99–111.
Raine, R., White, M., Dodge, J.D., 2002. The summer distribution of net plankton dinoflagellates and their relation to water movements in the NE Atlantic Ocean, west of Ireland. J. Plankton Res. 24, 1131–1147. https://doi.org/10.1093/plankt/24.11.1131.
Reverdin, G., Valdimarsson, H., Alory, G., Diverres, D., Bringas, F., Goni, G., Heilmann, L., Chafik, L., Szekely, T., Friedman, A.R., 2018. North Atlantic subpolar gyre along predetermined ship tracks since 1993: a monthly data set of surface temperature, salinity, and density. Earth Syst. Sci. Data 10, 1403–1415. https://doi.org/10.5194/essd-10-1403-2018.
Risebrobakken, B., Jansen, E., Andersson, C., Mjelde, E., Hevroy, K., 2003. A high-resolution study of Holocene paleoclimatic and paleoceanographic changes in the Nordic Seas. Paleoceanography 18, 1017. Artn 101710.1029/2002pa000764.
Risebrobakken, B., Dokken, T., Smedsrud, L.H., Andersson, C., Jansen, E., Moros, M., Ivanova, E.V., 2011. Early Holocene temperature variability in the Nordic Seas: the role of oceanic heat advection versus changes in orbital forcing. Paleoceanography 26, Pa4206. https://doi.org/10.1029/2011pa002117.
Rodriguez-Puebla, C., Encinas, A.H., Nieto, S., Garmendia, J., 1998. Spatial and temporal patterns of annual precipitation variability over the Iberian Peninsula. Int. J. Climatol. 18, 299–316. https://doi.org/10.1002/(Sici)1097-0088(19980315)18:3<299::Aid-Joc247>3.0.Co;2-L.
Rosenthal, Y., Boyle, E.A., Slowey, N., 1997. Temperature control on the incorporation

of magnesium, strontium, fluorine, and cadmium into benthic foraminiferal shells from Little Bahama Bank: prospects for thermocline paleoceanography. Geochem. Cosmochim. Acta 61, 3633–3643. https://doi.org/10.1016/S0016-7037(97)00181-6.

Rosenthal, Y., Field, M.P., Sherrell, R.M., 1999. Precise determination of element/calcium ratios in calcareous samples using sector field inductively coupled plasma mass spectrometry. Anal. Chem. 71, 3248–3253. https://doi.org/10.1021/ac981410x.

Rosenthal, Y., Morley, A., Barras, C., Katz, M.E., Jorissen, F., Reichart, G.J., Oppo, D.W., Linsley, B.K., 2011. Temperature calibration of Mg/Ca ratios in the intermediate water benthic foraminifer Hyalinea balthica. Geochem. Geophys. Geosyst. 12, Q04003. https://doi.org/10.1029/2010gc003333.

Ruprich-Robert, Y., Cassou, C., 2015. Combined influences of seasonal east Atlantic pattern and North Atlantic oscillation to excite atlantic multidecadal variability in a climate model. Clim. Dyn. 44, 229–253.

Scott, G.A., Scourse, J.D., Austin, W.E.N., 2003. The distribution of benthic foraminifera in the Celtic Sea: the significance of seasonal stratification. J. Foraminifer. Res. 33, 32–61. https://doi.org/10.2113/0330032.

Scourse, J., Austin, W., 2002. Quaternary Shelf Sea Palaeoceanography: Recent Developments in Europe. Elsevier.

Shackleton, N., 1974. Attainment of Isotopic Equilibrium between Ocean Water and the Benthonic Foraminifera Genus Uvigerina: Isotopic Changes in the Ocean during the Last Glacial.

Smedsrud, L.H., Esau, I., Ingvaldsen, R.B., Eldevik, T., Haugan, P.M., Li, C., Lien, V.S., Olsen, A., Omar, A.M., Ottera, O.H., Risebrobakken, B., Sando, A.B., Semenov, V.A., Sorokina, S.A., 2013. The role of the Barents Sea in the arctic climate system. Rev. Geophys. 51, 415–449. https://doi.org/10.1002/rog.20017.

Staines-Urias, F., Kuijpers, A., Korte, C., 2013. Evolution of subpolar North Atlantic surface circulation since the early Holocene inferred from planktic foraminifera faunal and stable isotope records. Quat. Sci. Rev. 76, 66–81. https://doi.org/10.1016/j.quascirev.2013.06.016.

Steele-Dunne, S., Lynch, P., McGrath, R., Semmler, T., Wang, S.Y., Hanafin, J., Nolan, P., 2008. The impacts of climate change on hydrology in Ireland. J. Hydrol. 356, 28–45. https://doi.org/10.1016/j.jhydrol.2008.03.025.

Stranne, C., Jakobsson, M., Bjork, G., 2014. Arctic ocean perennial sea ice breakdown during the early Holocene insolation maximum. Quat. Sci. Rev. 92, 123–132. https://doi.org/10.1016/j.quascirev.2013.10.022.

Stuiver, M., Reimer, P.J., 1993. Extended 14 C data base and revised CALIB 3.0 14 C age calibration program. Radiocarbon 35 (1), 215–230.

Sutton, R.T., Allen, M.R., 1997. Decadal predictability of North Atlantic sea surface temperature and climate. Nature 388, 563–567. https://doi.org/10.1038/41523.

Sweeney, J., 2014. Regional weather and climates of the British Isles–Part 6: Ireland. Weather 69, 20–27. https://doi.org/10.1002/wea.2230.

Thornalley, D.J., Elderfield, H., McCave, I.N., 2009. Holocene oscillations in temperature and salinity of the surface subpolar North Atlantic. Nature 457, 711–714. https://doi.org/10.1038/nature07717.

Tokinaga, H., Xie, S.P., Mukougawa, H., 2017. Early 20th-century Arctic warming intensified by Pacific and Atlantic multidecadal variability. Proc. Natl. Acad. Sci. U. S. A. 114, 6227–6232. https://doi.org/10.1073/pnas.1615880114.

Trenberth, K.E., Shea, D.J., 2006. Atlantic hurricanes and natural variability in 2005. Geophys. Res. Lett. 33, L12704 https://doi.org/10.1029/2006gl026894.

Trouet, V., Scourse, J.D., Raible, C.C., 2012. North Atlantic storminess and atlantic meridional overturning circulation during the last millennium: reconciling contradictory proxy records of NAO variability. Glob. Planet. Chang. 84–85, 48–55. https://doi.org/10.1016/j.gloplacha.2011.10.003.

Ulbrich, U., Christoph, M., 1999. A shift of the NAO and increasing storm track activity over Europe due to anthropogenic greenhouse gas forcing. Clim. Dyn. 15, 551–559.

Van Vliet, M., Ludwig, F., Zwolsman, J., Weedon, G., Kabat, P., 2011. Global river temperatures and sensitivity to atmospheric warming and changes in river flow. Water Resour. Res. 47.

Villanueva Guimerans, P., Cervera Currado, J.L., 1999. Distribution of Planorbulinacea (benthic Foraminifera) assemblages in surface sediments on the northern margin of the Gulf of Cadiz. Boletin. Inst. Espanol Oceanogr. 15, 181–190.

Vinther, B.M., Jones, P., Briffa, K., Clausen, H., Andersen, K., Dahl-Jensen, D., Johnsen, S., 2010. Climatic signals in multiple highly resolved stable isotope records from Greenland. Quat. Sci. Rev. 29, 522–538.

Walker, M., Head, M.H., Berklehammer, M., Bjorck, S., Cheng, H., Cwynar, L., Fisher, D., Gkinis, V., Long, A., Lowe, J., 2018. Formal Ratification of the Subdivision of the Holocene Series/Epoch (Quaternary System/Period): Two New Global Boundary Stratotype Sections and Points (GSSPs) and Three New Stages/subseries. Episodes.

Wallace, J.M., Gutzler, D.S., 1981. Teleconnections in the geopotential height field during the Northern Hemisphere winter. Mon. Weather Rev. 109, 784–812.

Wanner, H., Beer, J., Bütikofer, J., Crowley, T.J., Cubasch, U., Flückiger, J., Goosse, H., Grosjean, M., Joos, F., Kaplan, J.O., Küttel, M., Müller, S.A., Prentice, I.C., Solomina, O., Stocker, T.F., Tarasov, P., Wagner, M., Widmann, M., 2008. Mid- to Late Holocene climate change: an overview. Quat. Sci. Rev. 27, 1791–1828. https://doi.org/10.1016/j.quascirev.2008.06.013.

Wanner, H., Mercolli, L., Grosjean, M., Ritz, S.P., 2015. Holocene climate variability and change; a data-based review. J. Geol. Soc. 172, 254–263. https://doi.org/10.1144/jgs2013-101.

Woollings, T., Hannachi, A., Hoskins, B., 2010. Variability of the North Atlantic eddy-driven jet stream. Quart. J. Roy. Meteorol. Soc 136, 856–868. https://doi.org/10.1002/qj.625.

Yannick, M., Eynaud, F., Christophe, C., Rossignol, L., Brocheray, S., Mojtahid, M., Garcia, J., Peral, M., Howa, H., Zaragosi, S., 2017. Changes in Holocene meridional circulation and poleward Atlantic flow: the Bay of Biscay as a nodal point. Clim. Past 13, 201. https://doi.org/10.5194/cp-13-201-2017.

Zappa, G., Shaffrey, L.C., Hodges, K.I., Sansom, P.G., Stephenson, D.B., 2013. A multimodel assessment of future projections of North Atlantic and European extratropical cyclones in the CMIP5 climate models. J. Clim. 26, 5846–5862.

Zhang, R., Delworth, T.L., Held, I.M., 2007. Can the Atlantic Ocean drive the observed multidecadal variability in Northern Hemisphere mean temperature? Geophys. Res. Lett. 34.

Zhang, Q., Sundqvist, H.S., Moberg, A., Kornich, H., Nilsson, J., Holmgren, K., 2010. Climate change between the mid and late Holocene in northern high latitudes - Part 2: model-data comparisons. Clim. Past 6, 609–626. https://doi.org/10.5194/cp-6-609-2010.